Spine Deformity (2020) 8:537–546
https://doi.org/10.1007/s43390-020-00055-y

CASE SERIES

The effect of magnetically controlled growing rods on three-dimensional changes in deformity correction

Jason Pui Yin Cheung[1] · Prudence Wing Hang Cheung[1] · Kenneth M. C. Cheung[1]

Received: 21 August 2019 / Accepted: 16 November 2019 / Published online: 18 February 2020

Abstract

Study design Prospective radiographic study.

Objectives To determine the three-dimensional (3D) changes in deformity correction with magnetically controlled growing rod (MCGR) distractions.

Summary of background data MCGRs can achieve similar coronal plane correction as traditional growing rods. The changes in the sagittal and axial planes are unknown and should be studied as these factors reflect potential for proximal junctional kyphosis and rotational deformity. Frequent MCGR distractions may potentially improve axial plane deformities to the same extent as coronal and sagittal plane deformities.

Methods Early onset scoliosis (EOS) patients who underwent dual MCGRs with minimum 2-year follow-up were included in this study. 3D reconstructions of 6-monthly biplanar images were used to study changes in coronal, sagittal and axial planes. Changes in growth parameters (body height and arm span) were scaled to changes in coronal Cobb angles, sagittal profile (T1–12, T4–12, L1–L5, L1–S1), and rotational profile at the proximal thoracic, main thoracic and lumbar curves, and pelvic parameters (sagittal pelvic tilt, lateral pelvic tilt and pelvis rotation).

Results A total of 10 EOS patients were studied. The mean age at index surgery was 8.2 ± 3.0 years and mean postoperative follow-up of 34.3 ± 9.5 months. Six patients had rod exchange at mean 29.5 ± 11.8 months after initial implantation. Despite consistent gains in body height and arm span, the main changes in coronal and rotational profiles only occurred at the initial rod implantation surgery with only small changes occurring with subsequent follow-ups. Patients with higher preoperative proximal junctional angles had flattening of the sagittal plane occurring at initial surgery with early rebound. No changes in pelvic parameters were observed.

Conclusions The 3D changes with MCGR are mainly observed with initial rod implantation and no significant changes are observed with distractions. The MCGR can prevent deformity progression in the axial plane.

Level of evidence IV

Keywords Early onset scoliosis · Magnetically controlled growing rod · MCGR · 3D · Rotation · Axial

Introduction

Early onset scoliosis (EOS) requires early treatment as they occur in young children with significant remaining growth potential. Left untreated, these deformities are at risk of rapid progression, cosmetic disfigurement and pulmonary insufficiency [1–3]. Growing rods are one of the most common treatment methods for EOS that allow for physiological spine growth while preventing spine deformity progression [4–6]. Traditionally, these rods require open distraction surgeries every 6 months. However, repeated surgeries in a growing child have significant drawbacks including increased risk for anesthetic and wound complications [1, 7]. In response to these limitations, a remotely distractible magnetically controlled growing rod (MCGR) has been developed to allow for outpatient gradual lengthening [8]. The MCGR allows for safe distractions and continuous neurological monitoring in an awake patient. Clinical and radiological outcomes have been shown to be similar to traditional growing rods [8–15] and it has also been used

✉ Jason Pui Yin Cheung
cheungjp@hku.hk

[1] Department of Orthopaedics & Traumatology, The University of Hong Kong, Professorial Block, 5th Floor, 102 Pokfulam Road, Pokfulam, Hong Kong SAR, China

in safe gradual correction of severe spinal deformities [16, 17]. The MCGR also allows for non-invasive radiation-free monitoring [18, 19] and is an overall less costly option for EOS [20–22].

In terms of curve correction, most studies have showed that the largest amount of coronal curve correction occurs at implantation with subsequent satisfactory control of the deformity [8, 9, 12]. Despite these coronal changes, assessment of vertebral rotation is important for prognosis as scoliosis is a three-dimensional (3D) deformity [23–25]. The apical vertebral rotation (AVR) is particularly important with relevance to the rib hump which is a cosmetic concern. An increased rotational deformity may also lead to reduced chest cage area and thus pulmonary compromise. However, the changes in the axial plane with MCGR treatment is unknown due to limitations in imaging availability. Computed tomography (CT) measurements are most useful for measuring vertebral rotation as they provide the true rotational profile of the spine [26, 27]. However, it is not routinely performed in children due to high radiation exposure and lack of weight-bearing information.

Using the low-dose X-ray device EOS® (EOS® Imaging, Paris, France), we can obtain 3D reconstructed images of the spine based on biplanar images in posteroanterior (PA) and lateral standing views. The EOS® has already been shown to have good reliability for intraobserver and interobserver measurements for scoliosis curves with good precision (2°–4° variation only for vertebral rotation) [28–30]. Verification of the reconstructed 3D images with CT has already been performed and is shown to be reliable [31]. Thus, it is timely at this stage to assess the effect of gradual distractions with the MCGR on correction of vertebral rotation. 3D models of the spine are created to monitor the change in vertebral rotation with each distraction. This technique can also observe for any relationship between frequent distractions, spine length gain and transverse vertebral growth. Hence, the objective of this study is to determine the 3D corrections of EOS with MCGR distractions.

Materials and methods

Study design

This was a prospective radiographic study of patients with EOS who underwent dual MCGRs. Patients were recruited consecutively from a tertiary spine referral center since October 2015. None of the patients had prior treatment for their spinal deformity. All patients had major thoracic deformities, at least 2-year follow-up after their primary insertion of MCGRs, and images coupled with recorded body habitus parameters (body height, arm span, body weight). For all patients, dual MCGRs of 5.5 mm in diameter were placed in a standard and offset configuration to allow for the possibility for differential correction. Ethics was approved by the local institutional review board. All

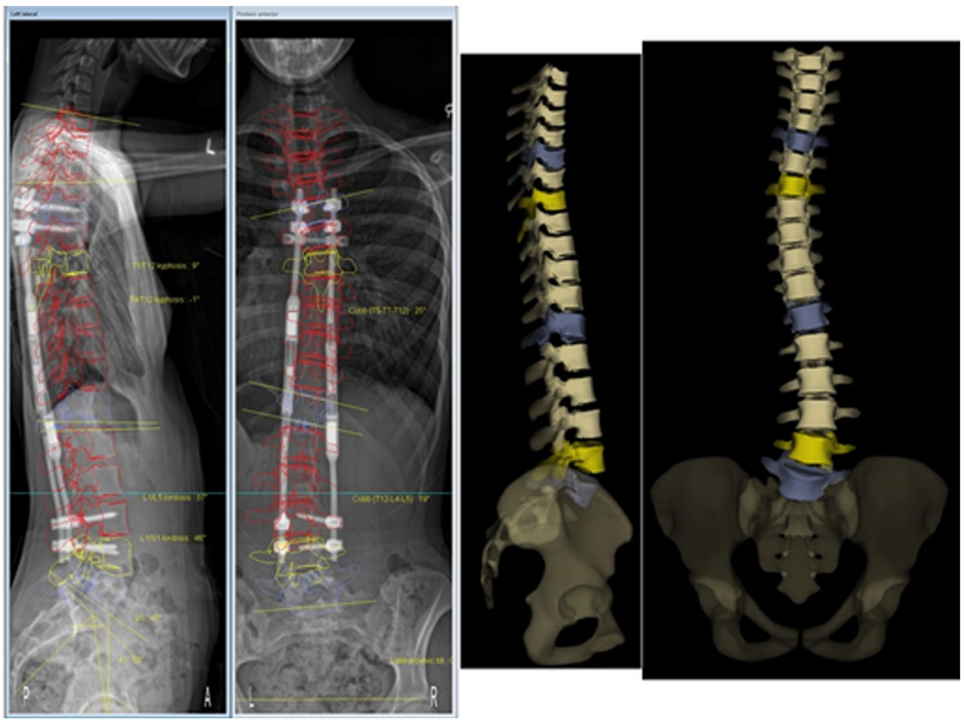

Fig. 1: 3D reconstruction output created from SterEOS®

patients underwent monthly 2-mm distractions to both rods starting at 2 months after MCGR implantation.

3D reconstruction

Radiographic images were obtained of recruited subjects using EOS® imaging every 6 months of follow-up to assess for longitudinal changes in parameters. The EOS® system is a slot-scanning radiographic device that utilizes two X-ray sources to allow simultaneous capture of both the PA and lateral images. It reduces the radiation to up to 9 times compared to conventional radiographs [32]. Two pairs of detectors are positioned, so that the images can be generated line by line as the scanning proceeds vertically. Patients stand in the machine, so images are taken in weight-bearing position. Scan time lasts for 8–15 s according to the patient's height. The reconstruction of the spine is based on available models provided by the EOS® company [29]. The image reconstruction procedure is as follows: Firstly, the pelvic anatomical landmarks are accessed. The two spheres of the acetabuli are identified as well as the sacral endplate. Then, the spinal curve from the T1 upper endplate to the L5 lower endplate is identified. The approximate borders of the spine vertebra are identified and a preliminary model is created. Fine adjustment of the model is performed by manipulating the points on the four corners of the vertebral body, pedicles and posterior arches from T1 to L5 [33]. Each modification improves the accuracy of the model. Finally, the accepted changes will create the 3D model with the necessary angles provided automatically (Fig. 1). The two-dimensional images

Table 1 Patient profiles

Subject number	Gender	Diagnosis	Age at MCGR implantation (years)	Foundations	Complications	Number of rod exchanges (years after first surgery)	Unplanned reoperation
#01	F	Juvenile idiopathic scoliosis	8.5	T4/5 upgoing pedicle hooks, L2/3 pedicle screws	Nil	1 (3 years)	
#02	F	Juvenile idiopathic scoliosis	12.7	T3/4 claw construct, L2/3 pedicle screws	Nil	0	
#03	F	Infantile idiopathic scoliosis with Marfanoid features	4.1	T4/5, L3/4 pedicle screws	Nil	1 (3 years)	
#04	F	Arthrogryposis	9.4	T3/4 upgoing pedicle hooks, L2/3 pedicle screws	Nil	0	
#05	F	Juvenile idiopathic scoliosis with Marfanoid features	7.4	T4/5, L3/4 pedicle screws	Proximal foundation nonunion, anchor loosening, bone formation at expandable portion of rod	1 (2 years)	2 (Proximal foundation nonunion and anchor loosening)
#06	F	Sotos syndrome	4.3	T5/6 claw construct, L3/4 pedicle screws	Bone formation at expandable portion of rod, metallosis	1 (4 years)	
#07	F	Juvenile idiopathic scoliosis	11.4	T5/6, L3/4 pedicle screws	Broken rod, metallosis	1 (2 years)	1 (Broken rod, metallosis)
#08	M	Neurofibromatosis scoliosis	4.8	T3/4, L3/4 pedicle screws	Infection	2 (2 years, 4 years)	1 (Infection)
#09	F	Neuromuscular scoliosis	10.4	T1/2, L1/2 pedicle screws	Nil	0	
#10	M	Juvenile idiopathic scoliosis	9.0	T5/6 upgoing pedicle hooks, L2/3 pedicle screws	Nil	0	

of the whole body had undergone 3D reconstructions of the spine and lower limb using the validated SterEOS®software (EOS® Imaging, Paris, France). Trained individuals blinded to the clinical information performed all image reconstructions. The time spent on 3D modeling was 31.7 ± 6.1 min per image reconstruction.

Study parameters

Demographic data including patient gender, age at MCGR implantation, and diagnosis (congenital, neuromuscular, syndromic, idiopathic) were recorded. Changes in body height (cm), body weight (kg), arm span (cm), and body mass index were recorded. Images were obtained preoperatively, immediate postoperatively, and from postoperative 6 months to postoperative 48 months at 6-monthly intervals. Details regarding the primary surgery included levels of instrumentation and anchor type (pedicle screw or hook). Any complications such as infection, anchor loosening, and proximal junctional kyphosis (PJK) were recorded. The number of rod exchanges was also recorded.

Specifically for the 3D imaging parameters, in addition to the gross morphology of the 3D model, the SterEOS® software provided the usually quoted spinopelvic alignment parameters [34]. These included the coronal Cobb angle, T1–T12 kyphosis, T4–T12 kyphosis, L1–S1 lordosis, L1–L5 lordosis, pelvic incidence, sagittal and lateral pelvic tilt, pelvic rotation and sacral slope. The rotational profile was also studied through the measurement of apical vertebral rotation at the thoracic apex, the proximal thoracic apex and the lumbar apex. PJK was identified by an increase in the proximal junctional angle (caudal endplate of the UIV to the cephalad endplate of two vertebrae proximally) of 10° or more and at least 10° greater than the preoperative measurement [35].

Statistical analysis

Descriptive statistics were calculated in mean, standard deviation (SD) and percentage. Mean values were plotted against follow-up time-points, enabling comparison between parameters. The timing of rod exchanges was also taken into account and was expressed using bar graphs within the dual-axis plot. Normality tests using Shapiro–Wilk tests were run and found that data were not normally distributed. One-way analysis of variance (ANOVA) was used to study the changes in radiographical parameters with time. Spearman correlation test was used to assess for any correlation between changes in the axial, coronal and sagittal parameters. Spearman's rank correlation coefficient (r_s) depicts the direction and strength of any relationships detected, with a value of 0.10–0.29 suggesting a small association; whereas a coefficient of 0.30–0.49 and ≥ 0.50 indicates a medium and a large association, respectively [36]. Statistical analyses were conducted using SPSS Windows 23.0 (IBM SPSS Inc., Chicago, Illinois, USA) and charts were created by Excel (Microsoft, Redmond, Washington, USA). A p value of < 0.05 was considered statistically significant.

Table 2 Baseline radiological parameters

Parameters	Mean ± SD
Imaging parameters	
Preoperative curve magnitude—Cobb angle (degrees)	
Thoracic	68.7 ± 18.3
Proximal thoracic	15.9 ± 20.6
Lumbar	39.7 ± 4.0
Proximal junctional angle	8.1 ± 4.6
Preoperative sagittal profile	
T1–T12 kyphosis	31.3 ± 13.3
T4–T12 kyphosis	29.0 ± 15.4
L1–S1 lordosis	58.0 ± 6.2
L1–L5 lordosis	41.5 ± 7.0
Preoperative pelvic profile	
Pelvic tilt	
Sagittal	4.7 ± 14.8
Lateral	7.0 ± 4.4
Pelvic incidence	48.6 ± 13.2
Sacral slope	43.9 ± 5.8
Pelvis rotation	− 1.0 ± 4.4
Preoperative rotational profile—apical vertebral rotation	
Thoracic apex	− 13.7 ± 10.5
Proximal thoracic apex	0.9 ± 1.4
Lumbar apex	5.2 ± 12.1

Results

A total of 10 (2 males, 8 females) EOS patients (Table 1) were studied. Their diagnoses were juvenile idiopathic ($n = 5$), infantile idiopathic ($n = 1$), neurofibromatosis ($n = 1$), neuromuscular (cerebral palsy GMFCS II, hypoxic brain injury at birth) ($n = 1$), Sotos syndrome ($n = 1$) and arthrogryposis ($n = 1$). The mean age at index surgery was 8.2 ± 3.0 years and the mean postoperative follow-up was 34.3 ± 9.5 months. Six patients had rod exchanges when the 4.8-cm distractable length was used up. The baseline profile of the patients is listed in Table 2. The preoperative body height was 122.7 ± 10.2 cm, preoperative arm span was 118.8 ± 12.8 cm, preoperative body weight was 20.8 ± 7.1 kg, and preoperative body mass index was 13.0 ± 2.9 kg/m^2. The pelvic incidence and lumbar lordosis were well matched preoperatively. No significant proximal thoracic deformity was observed in coronal, sagittal or axial planes.

Table 3 Changes of growth and clinical parameters between time-points

Parameters (mean ± SD)	Immediate postop vs preop	Postop 6 months vs immediate postop	12 vs 6 months	18 vs 12 months	24 vs 18 months	30 vs 24 months	36 vs 30 months	42 vs 36 months	48 vs 42 months	*p* Value
Changes of growth parameters mean ± SD)										
Body height (cm)	2.7 ± 1.5	2.0 ± 1.4	2.8 ± 0.5	3.4 ± 2.4	3.3 ± 1.2	3.8 ± 1.0	2.5 ± 0.6	1.3 ± 1.2	2.5 ± 2.1	0.371
Body weight (kg)	0.5 ± 0.7	2.0 ± 1.7	− 0.2 ± 1.0	1.5 ± 0.4	1.4 ± 2.2	1.4 ± 1.3	1.5 ± 1.9	1.6 ± 1.9	1.3 ± 1.5	0.765
Arm span (cm)	1.0 ± 0.0	4.0 ± 2.2	2.9 ± 0.9	2.8 ± 1.8	3.1 ± 1.1	3.3 ± 1.7	3.1 ± 1.5	1.0 ± 0.9	3.0 ± 0.0	0.004*
BMI	− 0.4 ± 0.6	0.7 ± 0.8	− 0.8 ± 0.6	0.1 ± 0.8	0.0 ± 0.9	0.1 ± 0.9	0.3 ± 0.9	0.4 ± 0.7	0.2 ± 0.4	0.785
Changes of Cobb angles (degree, mean ± SD)										
Thoracic	− 45.7 ± 24.4	3.5 ± 5.4	0.1 ± 1.3	1.3 ± 2.3	0.4 ± 4.0	− 2.2 ± 1.2	− 1.6 ± 3.5	0.6 ± 1.2	0.4 ± 1.6	< 0.001*
Proximal thoracic	− 12.7 ± 17.9	− 2.0 ± 3.0	− 0.4 ± 3.8	1.0 ± 3.8	0.2 ± 3.0	4.4 ± 3.1	0.5 ± 5.5	2.3 ± 4.4	3.6 ± 0.4	0.158
Lumbar	− 26.7 ± 7.1	2.3 ± 7.8	1.5 ± 3.5	− 1.7 ± 2.7	− 1.4 ± 0.4	− 1.8 ± 2.4	1.8 ± 3.3	− 0.5 ± 0.7	− 2.5 ± 3.5	< 0.001*
Proximal junctional angle	− 0.8 ± 3.6	2.6 ± 8.2	− 0.3 ± 4.0	0.0 ± 4.0	− 0.6 ± 3.6	0.4 ± 3.1	0.5 ± 2.7	− 1.8 ± 2.4	2.0 ± 2.8	0.532
Sagittal profile changes										
T1–T12 kyphosis	− 3.3 ± 1.4	8.2 ± 12.8	4.6 ± 7.8	2.8 ± 6.9	− 1.4 ± 5.0	− 3.2 ± 9.8	− 3.2 ± 6.4	4.7 ± 1.3	− 2.2 ± 5.7	0.393
T4–T12 kyphosis	− 6.2 ± 10.8	5.3 ± 8.0	4.5 ± 3.7	− 5.0 ± 2.0	1.6 ± 8.0	1.1 ± 2.5	0.9 ± 2.8	0.7 ± 4.5	1.5 ± 1.3	0.282
L1–S1 lordosis	− 10.4 ± 14.1	5.7 ± 10.3	6.6 ± 9.8	4.5 ± 4.8	− 2.6 ± 4.6	6.9 ± 8.0	− 3.9 ± 9.0	2.0 ± 3.3	1.0 ± 3.8	0.256
L1–L5 lordosis	− 7.3 ± 9.3	7.3 ± 4.2	2.8 ± 4.8	2.5 ± 4.0	− 0.2 ± 2.3	3.8 ± 4.0	− 1.1 ± 8.0	2.2 ± 1.6	0.6 ± 1.9	0.167
Rotational profile changes										
Thoracic apex	− 13.6 ± 11.4	1.5 ± 5.2	− 2.7 ± 5.1	1.2 ± 4.5	2.5 ± 5.6	− 1.6 ± 3.1	3.4 ± 3.5	− 1.3 ± 1.5	− 0.1 ± 1.1	0.042*
Proximal thoracic apex	− 1.1 ± 1.5	− 0.6 ± 7.3	2.1 ± 4.6	− 0.6 ± 5.2	− 1.4 ± 3.1	0.4 ± 9.5	− 0.2 ± 7.5	1.6 ± 2.3	− 2.1 ± 3.0	0.991
Lumbar apex	− 3.8 ± 2.0	4.3 ± 6.8	− 0.2 ± 5.4	− 1.6 ± 3.6	− 1.9 ± 5.1	1.4 ± 3.7	0.2 ± 2.6	1.0 ± 2.7	0.5 ± 0.7	0.574
Pelvic parameters (mean ± SD, degrees)										
Sagittal pelvic tilt	7.4 ± 10.7	− 4.0 ± 7.8	− 2.7 ± 10.3	− 2.4 ± 7.9	− 1.7 ± 7.1	− 0.6 ± 8.4	0.9 ± 8.8	0.3 ± 3.4	− 0.1 ± 6.8	0.903
Lateral pelvic tilt	2.0 ± 4.2	0.8 ± 1.7	− 0.3 ± 2.6	− 0.7 ± 1.2	0.3 ± 0.5	− 0.5 ± 2.1	0.0 ± 3.5	− 1.7 ± 1.2	2.5 ± 2.1	0.664
Pelvis rotation	6.3 ± 0.6	− 2.1 ± 9.0	0.5 ± 5.9	− 1.9 ± 1.4	2.4 ± 1.7	0.8 ± 1.5	0.2 ± 4.0	− 0.9 ± 2.2	3.0 ± 0.3	0.602

BMI body mass index

* indicates statistical significance $p < 0.05$

Consistent gains in body height, body weight, and arm span were observed with follow-up (Table 3). The main changes in coronal Cobb angles only occurred at the initial rod implantation surgery with only small changes that occurred at subsequent follow-ups. For the sagittal plane, the spine was flattened with initial surgery with reductions in T1–T12 and T4–T12 kyphosis, and L1–S1 and L1–L5 lordosis. There were rebound increases in kyphosis and lordosis within two years of follow-up followed by minimal changes thereafter. The lateral pelvic tilt maintained its position throughout follow-up; while, sagittal pelvic tilt gradually reduced to more retroversion especially in the first two years of follow-up. When comparing preoperative, immediate postoperative and final follow-up data (Table 4), the main changes only occurred for thoracic and lumbar Cobb angles, and L1-S1 lordosis.

For the axial plane, the apical vertebral rotation also had its largest change in the initial rod implantation without significant changes following subsequent distractions (Fig. 2) despite increasing body height. There was minimal change overall in the rotational profiles, even after rod exchanges. For the thoracic apex, which had the largest changes, besides the initial surgery, the maximum mean change was only 3.4 ± 3.5° thereafter. Similarly, the lumbar apex and proximal thoracic apex had maximal mean changes of 4.3 ± 6.8° and 3.4 ± 3.5°, respectively. Further analyses performed comparing the three parameters showed no significant correlations between coronal, sagittal and axial plane changes except for changes in coronal parameters and T1–L12 kyphosis and L1–L5 lordosis (Table 5).

None of our patients developed PJK. Analyzing the patients who had preoperatively larger proximal junctional angles (> 10°) showed flattening of their kyphotic angles with initial rod implantation (Table 6) but early rebound occurs within postoperative 6 months (Table 7).

Discussion

Understanding changes in 3D is crucial for proper management of patients with EOS. Rotational malalignment may aggravate the rib hump, which is a major concern for appearance. Increasing rotational deformities may also reduce the area of the chest cage thereby compromising pulmonary function. In this study, we explored the potential 3D changes that occur with MCGR treatment for EOS. Like the coronal Cobb angle, the main changes occur with the initial rod implantation without significant variations with distractions. Hence, the rotational profile is also maintained with MCGR treatment.

Axial plane rotation is commonly measured on plain radiographs by the Perdriolle and Vidal's method [37, 38]. However, 3D assessment based on a single two-dimensional image is inherently inaccurate as each scoliosis is unique with complexities that are not easily identified [39]. 3D reconstruction using the EOS® is accurate to within 4°–6° for the coronal deformity and 2°–4° for vertebral rotation

Table 4 Changes between preoperative, immediate postoperative and final follow-up measurements

Parameters	Mean preoperative (± SD)	Mean immediate postoperative (± SD)	Mean final follow-up (± SD)	Preoperative vs final *p* value	Immediate postop vs final *p* value
Cobb angle					
Thoracic	68.7 ± 18.3	23.8 ± 10.7	19.2 ± 9.6	0.005*	0.543
Proximal thoracic	15.9 ± 20.6	15.6 ± 13.8	18.5 ± 1.2	0.851	0.692
Lumbar	39.7 ± 4.0	9.1 ± 7.6	9.0 ± 8.2	0.002*	0.979
Proximal junctional angle	8.1 ± 4.6	7.3 ± 4.8	12.9 ± 8.7	0.359	0.322
Sagittal profile					
T1–T12 kyphosis	31.3 ± 13.3	33.5 ± 20.4	44.1 ± 16.7	0.327	0.451
T4–T12 kyphosis	29.0 ± 15.4	29.9 ± 17.2	33.3 ± 20.1	0.772	0.806
L1–S1 lordosis	58.0 ± 6.2	42.9 ± 18.8	44.1 ± 6.4	0.034*	0.912
L1–L5 lordosis	41.5 ± 7.0	30.3 ± 13.5	31.6 ± 7.3	0.130	0.876
Rotational Profile					
Thoracic apex	− 13.7 ± 10.5	− 11.2 ± 16.6	1.9 ± 15.5	0.197	0.292
Proximal thoracic apex	0.9 ± 1.4	1.5 ± 1.5	2.0 ± 5.4	0.748	0.864
Lumbar apex	5.2 ± 12.1	− 1.6 ± 5.3	8.6 ± 7.7	0.664	0.072
Pelvic parameters					
Sagittal pelvic tilt	4.7 ± 14.8	8.3 ± 13.7	6.8 ± 8.2	0.816	0.862
Lateral pelvic tilt	7.0 ± 4.4	5.3 ± 6.7	3.8 ± 1.3	0.325	0.673
Pelvis rotation	− 1.0 ± 4.4	0.7 ± 6.0	0.3 ± 4.9	0.742	0.916

* denotes statistical significance $p < 0.05$

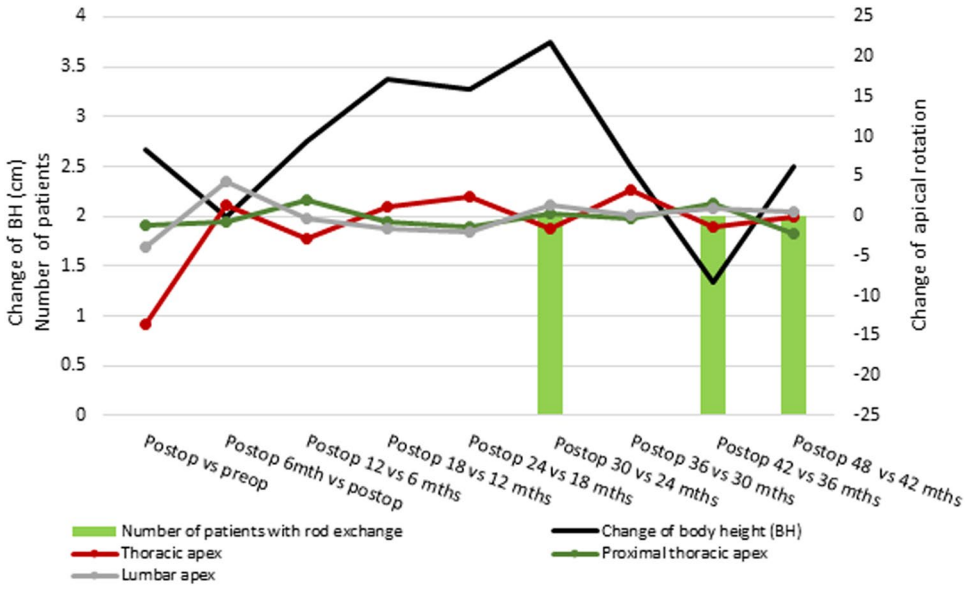

Fig. 2 Graph of the changes in rotational profile at the proximal thoracic, thoracic and lumbar apices with initial implantation and at every 6-month follow-up. The main change occurs at initial implantation and no significant deviations are observed thereafter despite growth or with rod exchange

in scoliosis [28, 29]. Verification of these reconstructed 3D images has been performed with CT and is proven to be reliable [31]. It is important to note that the time required to complete each 3D reconstruction was 31.7 ± 6.1 min. Despite the advantages of reduced radiation exposure, major drawbacks of using EOS® reconstructions are the manpower requirement and lack of automation which we hope will be solved in the future. Nevertheless, this is the best 3D assessment tool available currently.

The changes in the axial plane concerning growing rods are not well understood. Kamaci et al. [38] suggested that the apical vertebral rotation improves with traditional growing rod treatment by comparing the preoperative and final follow-up assessments. However, this does not reflect the changes occurring with distractions and the interplay with events like rod complications or rod exchanges. The 10° improvements reported in their study are similar to our findings of mean 13.6° reduction in rotation after MCGR implantation [38]. With the previous reports of similar initial corrections in the coronal plane after traditional growing rod and MCGR implantation [4, 9, 12–15], we speculate that the reported improvements elsewhere were contributed by the initial surgery rather than with distraction. Nevertheless, it is important to note that no deterioration in the rotational profile was observed during the course of the treatment. Hence, MCGR is successful in preventing axial plane deformity progression despite no anchors around the apex of the deformity.

The comparable changes found with rod implantation and with distractions in 3D are representative of spinal coupling [40–42]. Coupling indicates that changes in one plane is reflected upon the other planes. For example, initial MCGR implantation leads to coronal curve correction which is coupled with sagittal or axial plane changes. During MCGR implantation, no particular maneuver was performed to correct the apical rotation as there are only two sets of

Table 5 Correlation tests of changes in Cobb angles, sagittal parameters and rotational profiles at all time-points

	Coronal parameters							
	Thoracic Cobb angle		Proximal Thoracic Cobb angle		Lumbar Cobb angle		Proximal junctional angle	
Changes between time-points	r_s	p Value	r_s	p Value	r_s	p Value	r_s	p Value
Vertebral rotation at thoracic apex	0.191	0.320	0.278	0.145	0.228	0.235	−0.094	0.626
Sagittal parameters								
T1–T12 kyphosis	0.496	0.006**	−0.210	0.274	0.116	0.550	−0.198	0.304
T4–T12 kyphosis	0.174	0.368	−0.359	0.056	0.286	0.133	0.184	0.339
L1–S1 lordosis	0.406	0.029*	0.042	0.831	−0.080	0.681	0.138	0.475
L1–L5 lordosis	0.330	0.081	−0.074	0.701	−0.098	0.613	−0.370	0.048*

* denotes statistical significance $p < 0.05$

anchors placed at the proximal and distal foundations without any instrumentation in the intervening spinal segments or attempt to derotate the spine. Hence, effectively, only the coronal deformity is planned for correction with rod insertion and intraoperative distraction maneuvers. The spontaneous reduction of the rotational deformity is achieved through coupling.

An interesting phenomenon is observed for the sagittal plane. Proper contouring of the MCGR is not easily achievable due to the straight actuator segment [12, 30]. This has been attributed to the high risk of PJK after growing rod surgery [30, 43, 44]. The ability of the spine to compensate for sudden flattening of the sagittal alignment is highlighted by the early rebound in thoracic kyphosis and lumbar lordosis after rod implantation. Interestingly, we did not observe any cases with PJK even with the larger preoperative higher proximal junctional angles. There is recruitment of more cranial spinal segments to reproduce the thoracic kyphosis and is clearly represented by a rebound increase in proximal junctional angle as early as postoperative 6 months. There is also greater T1–T12 kyphotic change as compared to T4–T12. The inclusion of T1–4 in addition to the T4–T12 better incorporates the kyphotic changes occurring in the proximal thoracic spinal segments. In our series, the increase in kyphosis was only observed in the early postoperative follow-up and the overall kyphosis did not change thereafter. There is no further deterioration in the proximal junctional angle after the early change. This may be a reason why we did not observe PJK in our series as compared to previous reports (~40%) [15, 43].

There are several limitations to this study that must be discussed. Firstly, we report the results of a small number of patients with variable ages at rod implantation. The lack of significance reported by the correlation analyses may be related to these limitations. However, it may also represent the variations in 3D curve types that have been reported [39]. For example, not all scoliosis curves are hypokyphotic and as correlation analyses are uni-directional, this tool may not be most representative of interactions between coronal, sagittal and axial planes. Nevertheless, our results will need to be validated in a larger study. For the purposes of this study, despite the presence of implants superimposing onto the vertebral bodies, measurements using the EOS® are still possible for postoperative images with reproducible data [34]. However, in one study investigating 3D reconstructions of the spine with posterior instrumentation in situ, the reported precision may vary from 2.8° to 10° for Cobb angles and 6.8° to 10.4° for apical vertebral rotation calculations. At present, we unfortunately have no other more accurate 3D assessment available for children which also avoids the high radiation exposure associated with CT.

This is the first study to assess 3D changes in scoliosis correction with MCGR distractions. The corrections in

Table 6 Proximal junctional angle (mean values ± SD) at specific time-points

PJA	Preoperative	Immediate PO	PO 6 months	PO 12 months	PO 18 months	PO 24 months	PO 30 months	PO 36 months	PO 42 months	PO 48 months
> 10° ($n=3$)	12.3 ± 5.3	7.7 ± 8.8	18.8 ± 19.4	19.5 ± 14.4	20.3 ± 7.6	18.5 ± 5.0	19.6 ± 6.1	20.2 ± 5.1	16.1 ± 3.6	20.3 ± 4.2
< 10° ($n=7$)	6.3 ± 3.0	7.2 ± 3.1	6.1 ± 5.3	5.4 ± 3.9	5.0 ± 3.8	5.2 ± 3.1	5.3 ± 3.5	5.8 ± 1.8	5.2 ± 0.8	5.5 ± 2.3
p Value	0.067	0.667	0.517	0.183	0.033*	0.024*	0.024*	0.024*	0.024*	0.100

PJA proximal junctional angle, *PO* postoperative
* denotes statistical significance $p < 0.05$

Table 7 Changes in Proximal junctional angle (mean values ± SD) at specific time-points

PJA	Preop vs Immediate PO	PO 6 months vs Immediate PO	PO 12 vs 6 months	PO 18 vs 12 months	PO 24 vs 18 months	PO 30 vs 24 months	PO 36 v 30 months	PO 42 vs 36 months	PO 48 vs 42 months
> 10° ($n=3$)	−4.6 ± 3.7	11.1 ± 10.8	0.7 ± 6.4	0.8 ± 6.8	−1.8 ± 6.5	1.1 ± 6.0	0.6 ± 3.3	−4.1 ± 1.5	4.2 ± 0.6
< 10° ($n=7$)	0.9 ± 2.1	−1.1 ± 3.3	−0.7 ± 3.1	−0.4 ± 2.8	0.0 ± 1.8	0.1 ± 0.9	0.5 ± 2.7	−0.6 ± 1.8	−0.2 ± 2.4
p Value	0.033*	0.033*	0.517	0.833	0.714	1.000	1.000	0.048*	0.100

PJA proximal junctional angle, *PO* postoperative

* denotes statistical significance $p < 0.05$

rotational deformity are seen only with initial rod implantation and no significant changes are observed with distractions thereafter. Hence, the MCGR is successful in controlling the deformity and prevents its progression in the coronal, sagittal and axial planes. Understanding 3D changes in the deformity is important as it provides insight into how growth-sparing distraction devices can be tailored towards different patients with variable curve types. Further study can examine whether transverse plane growth deviates with MCGR treatment and whether this influences the correction outcomes achieved at final fusion surgery, as well as correlation with respiratory function.

Key points

- The rotational correction is greatest with the initial magnetically controlled growing rod implantation and is stable thereafter with distractions.
- Patients with higher preoperative proximal junctional angles had flattening of the sagittal alignment with rod implantation followed by early rebound.
- No significant changes in coronal, sagittal or axial plane deformities occur with distractions up to 4-year follow-up.

Author contributions JPYC—Study conception and design, data acquisition, analysis, interpretation of data, drafting manuscript. PWHC—Data acquisition and analysis, interpretation of data, revising manuscript. KMCC—Interpretation of data, revising manuscript. All authors approved the final version of the manuscript.

Funding This study was supported by the Scoliosis Research Society.

Compliance with ethical standards

Conflict of interests The authors have no financial or competing interests to disclose.

Ethical approval Permission to reproduce copyrighted materials or signed patient consent forms granted. The study was approved by the local institutional review board (UW 16-336).

References

1. Akbarnia BA, Emans JB (2010) Complications of growth-sparing surgery in early onset scoliosis. Spine (Phila Pa 1976) 35:2193–2204
2. Bess S, Akbarnia BA, Thompson GH et al (2010) Complications of growing-rod treatment for early-onset scoliosis: analysis of one hundred and forty patients. J Bone Joint Surg Am 92:2533–2543
3. Redding GJ, Mayer OH (2011) Structure-respiration function relationships before and after surgical treatment of early-onset scoliosis. Clin Orthop Relat Res 469:1330–1334
4. Akbarnia BA, Breakwell LM, Marks DS et al (2008) Dual growing rod technique followed for three to eleven years until final fusion: the effect of frequency of lengthening. Spine (Phila Pa 1976) 33:984–990
5. Akbarnia BA, Marks DS, Boachie-Adjei O, Thompson AG, Asher MA (2005) Dual growing rod technique for the treatment of progressive early-onset scoliosis: a multicenter study. Spine (Phila Pa 1976) 30:S46–57
6. Winter RB, Moe JH, Lonstein JE (1984) Posterior spinal arthrodesis for congenital scoliosis. An analysis of the cases of two hundred and ninety patients, five to nineteen years old. J Bone Joint Surg Am 66:1188–1197
7. Bess S, Akbarnia BA, Thompson GH et al (2011) Complications of growing-rod treatment for early-onset scoliosis: analysis of one hundred and forty patients. J Bone Joint Surg Am 92:2533–2543
8. Cheung KM, Cheung JP, Samartzis D et al (2012) Magnetically controlled growing rods for severe spinal curvature in young children: a prospective case series. Lancet 379:1967–1974
9. Akbarnia BA, Cheung K, Noordeen H et al (2013) Next generation of growth-sparing techniques: preliminary clinical results of a magnetically controlled growing rod in 14 patients with early-onset scoliosis. Spine (Phila Pa 1976) 38:665–670
10. Cheung JP, Cheung KM (2019) Current status of the magnetically controlled growing rod in treatment of early-onset scoliosis: what we know after a decade of experience. J Orthop Surg 27:2309499019886945
11. Cheung JP, Cahill P, Yaszay B, Akbarnia BA, Cheung KM (2015) Special article: update on the magnetically controlled growing rod: tips and pitfalls. J Orthop Surg (Hong Kong) 23:383–390
12. Cheung JPY, Yiu K, Kwan K, Cheung KMC (2019) Mean 6-year follow-up of magnetically controlled growing rod patients with

early onset scoliosis: a glimpse of what happens to graduates. Neurosurgery 84:1112–1123
13. Cheung JPY, Yiu KKL, Samartzis D, Kwan K, Tan BB, Cheung KMC (2018) Rod lengthening with the magnetically controlled growing rod: factors influencing rod slippage and reduced gains during distractions. Spine (Phila Pa 1976) 43:E399–E405
14. Heydar AM, Sirazi S, Bezer M (2016) Magnetic controlled growing rods (MCGR) As a treatment of early onset scoliosis (EOS): early results with two patients had been fused. Spine (Phila Pa 1976) 41:E1336–E1342
15. Teoh KH, Winson DM, James SH et al (2016) Magnetic controlled growing rods for early-onset scoliosis: a 4-year follow-up. Spine J 16:S34–S39
16. Cheung JP, Samartzis D, Cheung KM (2014) A novel approach to gradual correction of severe spinal deformity in a pediatric patient using the magnetically-controlled growing rod. Spine J 14:e7–13
17. Kwan KYH, Cheung JPY, Yiu KKL, Cheung KMC (2018) Ten year follow-up of Jarcho-Levin syndrome with thoracic insufficiency treated by VEPTR and MCGR VEPTR hybrid. Eur Spine J 27:287–291
18. Cheung JP, Bow C, Samartzis D, Ganal-Antonio AK, Cheung KM (2016) Clinical utility of ultrasound to prospectively monitor distraction of magnetically controlled growing rods. Spine J 16:204–209
19. Cheung JPY, Yiu KKL, Bow C, Cheung PWH, Samartzis D, Cheung KMC (2017) Learning curve in monitoring magnetically controlled growing rod distractions with ultrasound. Spine (Phila Pa 1976) 42:1289–1294
20. Charroin C, Abelin-Genevois K, Cunin V et al (2014) Direct costs associated with the management of progressive early onset scoliosis: estimations based on gold standard technique or with magnetically controlled growing rods. Orthop Traumatol Surg Res 100:469–474
21. Rushton PRP, Siddique I, Crawford R, Birch N, Gibson MJ, Hutton MJ (2017) Magnetically controlled growing rods in the treatment of early-onset scoliosis: a note of caution. Bone Joint J 99:708–713
22. Wong CKH, Cheung JPY, Cheung PWH, Lam CLK, Cheung KMC (2017) Traditional growing rod versus magnetically controlled growing rod for treatment of early onset scoliosis: cost analysis from implantation till skeletal maturity. J Orthop Surg (Hong Kong) 25:2309499017705022
23. Gunzburg R, Gunzburg J, Wagner J, Fraser RD (1991) Radiologic interpretation of lumbar vertebral rotation. Spine 16:660–664
24. Lopez-Sosa F, Guille JT, Bowen JR (1995) Rotation of the spine in congenital scoliosis. J Pediatr Orthop 15:528–534
25. Perdriolle R, Vidal J (1985) Thoracic idiopathic scoliosis curve evolution and prognosis. Spine (Phila Pa 1976) 10:785–791
26. Krismer M, Sterzinger W, Haid C, Frischhut B, Bauer R (1996) Axial rotation measurement of scoliotic vertebrae by means of computed tomography scans. Spine (Phila Pa 1976) 21:576–581
27. Lam GC, Hill DL, Le LH, Raso JV, Lou EH (2008) Vertebral rotation measurement: a summary and comparison of common radiographic and CT methods. Scoliosis 3:16
28. Gille O, Champain N, Benchikh-El-Fegoun A, Vital JM, Skalli W (2007) Reliability of 3D reconstruction of the spine of mild scoliotic patients. Spine (Phila Pa 1976) 32:568–573
29. Humbert L, De Guise JA, Aubert B, Godbout B, Skalli W (2009) 3D reconstruction of the spine from biplanar X-rays using parametric models based on transversal and longitudinal inferences. Med Eng Phys 31:681–687
30. Obid P, Yiu KKL, Cheung KM, Kwan K, Ruf M, Cheung JPY (2018) Reliability of rod lengthening, thoracic, and spino-pelvic measurements on biplanar stereoradiography in patients treated with magnetically controlled growing rods. Spine (Phila Pa 1976) 43:1579–1585
31. Glaser DA, Doan J, Newton PO (2012) Comparison of 3-dimensional spinal reconstruction accuracy: biplanar radiographs with EOS versus computed tomography. Spine (Phila Pa 1976) 37:1391–1397
32. Deschenes S, Charron G, Beaudoin G et al (2010) Diagnostic imaging of spinal deformities: reducing patients radiation dose with a new slot-scanning X-ray imager. Spine (Phila Pa 1976) 35:989–994
33. Pomero V, Mitton D, Laporte S, de Guise JA, Skalli W (2004) Fast accurate stereoradiographic 3D-reconstruction of the spine using a combined geometric and statistic model. Clin Biomech (Bristol, Avon) 19:240–247
34. Ilharreborde B, Steffen JS, Nectoux E et al (2011) Angle measurement reproducibility using EOS three-dimensional reconstructions in adolescent idiopathic scoliosis treated by posterior instrumentation. Spine (Phila Pa 1976) 36:E1306–E1313
35. Glattes RC, Bridwell KH, Lenke LG, Kim YJ, Rinella A, Edwards C 2nd (2005) Proximal junctional kyphosis in adult spinal deformity following long instrumented posterior spinal fusion: incidence, outcomes, and risk factor analysis. Spine (Phila Pa 1976) 30:1643–1649
36. Cohen J, Cohen P, West SG, Aiken LS (2003) Applied multiple regression/correlation analysis for the behavioral sciences, 3rd edn. Lawrence Erlbaum Associates, Hillsdale
37. Acaroglu E, Yazici M, Alanay A, Surat A (2002) Three-dimensional evolution of scoliotic curve during instrumentation without fusion in young children. J Pediatr Orthop 22:492–496
38. Kamaci S, Demirkiran G, Ismayilov V, Olgun ZD, Yazici M (2014) The effect of dual growing rod instrumentation on the apical vertebral rotation in early-onset idiopathic scoliosis. J Pediatr Orthop 34:607–612
39. Sangole AP, Aubin CE, Labelle H et al (2009) Three-dimensional classification of thoracic scoliotic curves. Spine (Phila Pa 1976) 34:91–99
40. Luk KD, Cheung WY, Wong Y, Cheung KM, Wong YW, Samartzis D (2012) The predictive value of the fulcrum bending radiograph in spontaneous apical vertebral derotation in adolescent idiopathic scoliosis. Spine (Phila Pa 1976) 37:E922–E926
41. Luk KD, Vidyadhara S, Lu DS, Wong YW, Cheung WY, Cheung KM (2010) Coupling between sagittal and frontal plane deformity correction in idiopathic thoracic scoliosis and its relationship with postoperative sagittal alignment. Spine (Phila Pa 1976) 35:1158–1164
42. Yao G, Cheung JPY, Shigematsu H et al (2017) Characterization and predictive value of segmental curve flexibility in adolescent idiopathic scoliosis patients. Spine (Phila Pa 1976) 42:1622–1628
43. Kwan KYH, Alanay A, Yazici M et al (2017) Unplanned reoperations in magnetically controlled growing rod surgery for early onset scoliosis with a minimum of two-year follow-Up. Spine (Phila Pa 1976) 42:E1410–E1414
44. Lebon J, Batailler C, Wargny M et al (2017) Magnetically controlled growing rod in early onset scoliosis: a 30-case multicenter study. Eur Spine J 26:1567–1576